Available online at www.sciencedirect.com

ScienceDirect

Journal of Power Sources 170 (2007) 130–139

JOURNAL OF POWER SOURCES

www.elsevier.com/locate/jpowsour

Analysis of the design of a pressurized SOFC hybrid system using a fixed gas turbine design

S.K. Park, K.S. Oh, T.S. Kim*

Department of Mechanical Engineering, Inha University, 253 Yonghyun-Dong,
Nam-Gu, Incheon 402-751, Republic of Korea

Received 26 December 2006; received in revised form 16 March 2007; accepted 29 March 2007

Abstract

Design characteristics and performance of a pressurized solid oxide fuel cell (SOFC) hybrid system using a fixed gas turbine (GT) design are analyzed. The gas turbine is assumed to exist prior to the hybrid system design and all the other components such as the SOFC module and auxiliary parts are assumed to be newly designed for the hybrid system. The off-design operation of the GT is modeled by the performance characteristics of the compressor and the turbine. In the SOFC module, internal reforming with anode gas recirculation is adopted. Variations of both the hybrid system performance and operating condition of the gas turbine with the design temperature of the SOFC were investigated. Special focus is directed on the shift of the gas turbine operating points from the original points. It is found that pressure loss at the fuel cell module and other components, located between the compressor and the turbine, shifts the operating point. This results in a decrease of the turbine inlet temperature at each compressor operating condition relative to the original temperature for the GT only system. Thus, it is difficult to obtain the original GT power. Two cell voltage cases and various degrees of temperature difference at the cell are considered and their influences on the system design characteristics and performance are comparatively analyzed.

Keywords: Solid oxide fuel cell; Gas turbine; Pressurized hybrid system; Pressure loss; Compressor surge

1. Introduction

The solid oxide fuel cell (SOFC) is considered a suitable candidate for the electric power plant applications. One of its attractive features is high operating temperature (600–1000 °C), which allows favorable combination with other types of power generators such as gas turbines (GTs). R&D efforts pertaining to SOFC/GT hybrid systems have been initiated worldwide and a few systems are under development for commercialization [1]. The thermodynamic synergy effect of combining the SOFC and the GT can be most effectively realized when the SOFC is designed to operate at an elevated pressure. This kind of system is called a pressurized system where pressurized air from the compressor is delivered directly to the SOFC and the outgoing high pressure gas drives the turbine. This design can be considered to be a modification of a fuel cell only system in that the original air blower is replaced by a compressor which enables a higher operating pressure and thus guarantees higher cell voltage. The turbine is added to recover the high pressure energy of the gas exhausted from the cell. This turbine expansion plays a dominant role in enhancing the efficiency of the entire system [2]. The pressurized system also allows for compact design of auxiliary equipments such as piping due to the relatively high pressure at those parts. Another means of combining the SOFC and GT is an ambient pressure system where the cell operates at a near ambient pressure. This system also has several advantages, the most prominent of which is selection of the GT pressure independently of the cell pressure. Aside from practical cons and pros involved in realizing the two types of system configurations, many basic studies have concluded that a pressurized system may have higher system efficiency over an ambient pressure system from a thermodynamic point of view if equivalent design parameters are assumed [3]. Recent development examples of commercial SOFC/GT hybrid systems have also adopted the pressurized configuration [4,5].

---

* Corresponding author. Tel.: +82 32 860 7307; fax: +82 32 868 1716.
E-mail addresses: waitingme79@hanmail.net (S.K. Park), seeone@hanmail.net (K.S. Oh), kts@inha.ac.kr (T.S. Kim).

0378-7753/$ – see front matter © 2007 Elsevier B.V. All rights reserved.
doi:10.1016/j.jpowsour.2007.03.067

Nomenclature

CIT	cathode inlet temperature (°C)
CDP	compressor discharge pressure (kPa)
E	electric potential (V)
F	Faraday constant
FCT	fuel cell temperature (°C)
$\bar{h}$	molar enthalpy (kJ kmol^{-1})
I	current (A)
J	current density (A m^{-2})
L	thickness (m)
LHV	lower heating value (kJ kg^{-1})
$\dot{m}$	mass flow rate (kg s^{-1})
$\dot{n}$	molar flow rate (kmol s^{-1})
P	pressure (kPa)
$\dot{Q}$	heat transfer rate (kW)
T	temperature (°C)
ΔT_c	temperature difference at the cell (°C)
TIT	turbine inlet temperature (°C)
V	cell voltage (V)
$\dot{W}$	power (kW)
Greek letters	
ε	heat exchanger effectiveness
η	efficiency
ρ	resistance (Ω m)
Subscripts	
a	anode, air
ac	alternating current
AUX	auxiliary equipment
C	compressor
c	cathode, cold side
conv	conversion
dc	direct current
e	electrolyte
FC	fuel cell
gen	generator
GT	gas turbine
h	hot side
HS	hybrid system
i	component
in	inlet
m	mechanical
N	Nernst
out	outlet
P	polarization
r	reformer
ref	reference
T	turbine

Recently, diverse analysis results on the design performance of pressurized SOFC hybrid systems considering various options in combining the SOFC and the GT have been reported. Examples include fundamental design parametric analyses [6,7], a study on the influence of the reforming method [8], an investigation into the influences of both reforming method and temperature constraints on the cell [9]. Most of the design analyses have been performed under the assumption that all components including the SOFC, the GT, and balance-of-the-plant (BOP) parts can be manufactured as predicted. In particular, smoothly matched design of the SOFC and the GT is generally assumed to be possible, that is, a sub-system (GT or SOFC) is assumed to be designed to match the design of the other subsystem. In many studies, parameters of the GT, such as power and main component parameters including turbine inlet temperature, pressure ratio and air flow rate, which match the given design parameters of the SOFC stack (the cell temperature, etc.), have been obtained as a result of analysis. This analysis seems logical in that the SOFC is the major component that generates greater power than the GT. The underlying assumption of this analysis is that the gas turbine, exactly matching the analysis requirements, is available as an off-the-shelf item or the gas turbine is to be newly designed and manufactured to match the design specifications. However, the assumption is rather unreasonable in reality. A gas turbine that exactly matches the required design specifications of the analysis is not usually available as an off-the-self item. Moreover, a new design, i.e. development of a new gas turbine, is generally prohibitive in terms of cost. On the other hand, the capacity (power) of SOFC can be determined more flexibly due to the possibility of modular design of the fuel cell stack, which is one of the most advantageous features of the fuel cell. Accordingly, the design of a hybrid system based on an existing (commercially available) gas turbine is more practical as a short- or mid-term development strategy. An example about predicting system design and operation of a hybrid system based on a commercially available GT can be found in the literature [10].

In a pressurized hybrid system, the turbine inlet state is directly affected by the thermo-fluid dynamic operating conditions of the components located between the compressor and the turbine, such as the SOFC stack and piping. Therefore, the operating conditions of the gas turbine are different from those of the original GT only system. A previous work [11], in which the operational characteristics of an experimental hybrid system simulator were investigated, reported that operation of the compressor during start-up approaches the surge condition. This might have been caused by the change of the GT operation conditions from the original conditions. The possibility of the compressor surge during transient operation for a hybrid system designed at near surge condition has also been reported [12]. Therefore, the design operation condition should be sufficiently far from the surge condition (large surge margin), and this limitation may provide a critical constraint in designing a pressurized hybrid system based on an existing gas turbine.

The aim of this study is to simulate the design of a pressurized SOFC hybrid system using an existing (fixed) gas turbine and to provide useful fundamental design characteristics as well as potential critical problems. The gas turbine is assumed to exist prior to the hybrid system design and all the other components such as SOFC module and auxiliary parts are assumed to be newly designed for the hybrid system. Special focus is given to the shift of the compressor operating points from the original gas turbine design point depending on the design cell temperature. In order to examine the matching characteristic of the gas turbine with different design practices of the fuel cell, a wide range of cell design temperature is used. Thus, this study presents rather general design results using different fuel cell designs. Researchers or designers may refer to the result that includes design conditions closest to their cell design practices. The influence of the cell voltage on the design characteristics and performance is examined as well. Also, since the temperature difference at the cell is an important design parameter that affects not only the SOFC performance but also the hybrid system performance [3,9], its effect on integration of the SOFC and the existing GT is investigated.

2. Analysis

2.1. System configuration

Fig. 1 shows the hybrid system configuration analyzed in this study. This system is conceptually similar to that used in a demonstration project [4]. The SOFC module includes a cell stack, a reformer, an afterburner and a preheater. Internal reforming is adopted, and the steam required for the reforming reaction is supplied by the anode gas recirculation. The compressed air is heated consecutively through a recuperator and a preheater and then flows into the cathode of the SOFC. The remaining fuel from the anode is combusted with the cathode exit air at the afterburner. The high temperature gas supplies heat to the preheater to meet the required cathode inlet temperature and then flows into the turbine. The turbine exit gas heats up the fuel and the compressor discharge air.

2.2. Modeling and analysis

The gas turbine is assumed to be a single-shaft micro gas turbine equipped with a centrifugal compressor and a radial turbine. The design compressor pressure ratio is 4.6 and the turbine inlet temperature is 950 °C. Turbine blade cooling is not considered. The design mass flow of 1.0 kg s^{-1} is assumed to produce roughly 120 kW power. The design specifications of the gas turbine are summarized in Table 1. Based on the gas turbine design specifications given prior to the hybrid system design, design of a hybrid system requires simulation of the off-design operation of the gas turbine. The gas turbine off-design operation is simulated with the aid of the performance characteristics of the compressor and the turbine. The compressor characteristics are described by a performance map as will be shown in the results. The turbine is modeled by the following Stodola equation [13], which was proved to closely represent the turbine running line of a micro gas turbine [14].

Table 1
Design parameters of the gas turbine

Ambient condition	101.3 kPa, 15 °C
Air flow rate	1.0 kg s^{-1}
Compressor pressure ratio	4.6
Compressor efficiency	0.75
Turbine inlet temperature	950 °C
Turbine efficiency	0.85
Recuperator effectiveness	0.83
Shaft speed	65,000 rpm
Generator efficiency	0.93
Combustor pressure loss	3%
Recuperator pressure losses	Cold side 1.5%, hot side 2.5%
Duct pressure losses	0.5%

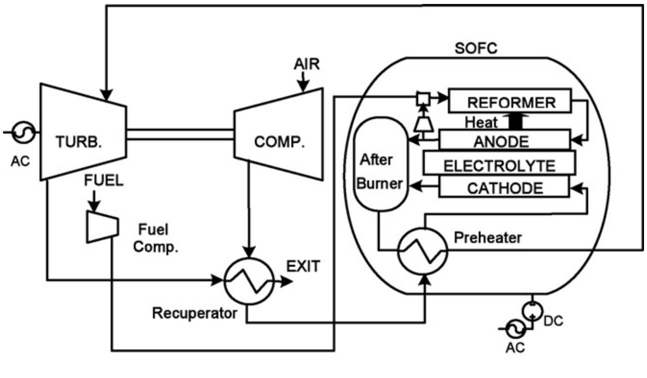

Fig. 1. Configuration of the pressurized SOFC/GT hybrid system.

$$\frac{\dot{m}_{\text{in}}\sqrt{T_{\text{in}}}/P_{\text{in}}}{\left(\dot{m}_{\text{in}}\sqrt{T_{\text{in}}}/P_{\text{in}}\right)_{\text{ref}}} = \frac{\sqrt{1-(P_{\text{out}}/P_{\text{in}})^2}}{\sqrt{1-(P_{\text{out}}/P_{\text{in}})_{\text{ref}}^2}} \tag{1}$$

All parameters are those of the turbine inlet and outlet, and the reference point is the turbine design point. Except for the gas turbine components, all the other parts including the SOFC module are assumed to be newly designed for the hybrid system. Each component is modeled as a lumped control volume. The fuel is methane and the steam reforming reaction and the water gas shift reaction are assumed to take place at equilibrium. The amount of steam supplied to the reformer is determined by the steam carbon ratio, defined as the ratio between the supplied steam to the cell and the supplied methane. Both hydrogen and carbon monoxide generated by the steam reforming process participate in the electrochemical reactions:

$$\mathrm{H_2} + \tfrac{1}{2}\mathrm{O_2} \rightarrow \mathrm{H_2O} \tag{2a}$$

$$\mathrm{CO} + \tfrac{1}{2}\mathrm{O_2} \rightarrow \mathrm{CO_2} \tag{2b}$$

The fuel utilization factor at the cell is defined as the ratio between reacted and supplied fuel at the cell (hydrogen and carbon monoxide).

Concerning the design of the SOFC stack module, it is assumed that the current density of the unit cell is the same for all design conditions. A different power requirement obtained from the analysis can be satisfied by modification of the unit cell configuration and/or cell stack size (eg. number of stacked cells). Two case studies have been investigated regarding the cell voltage behavior as a function of temperature. In the first case, a variation of the cell voltage with the cell operating temperature is adopted. The cell voltage is predicted by subtracting various losses from the Nernst potential as follows.

$$V = E_{\text{N}} - E_{\text{P}} - J(\rho_{\text{a}}L_{\text{a}} + \rho_{\text{e}}L_{\text{e}} + \rho_{\text{c}}L_{\text{c}}) \tag{3}$$

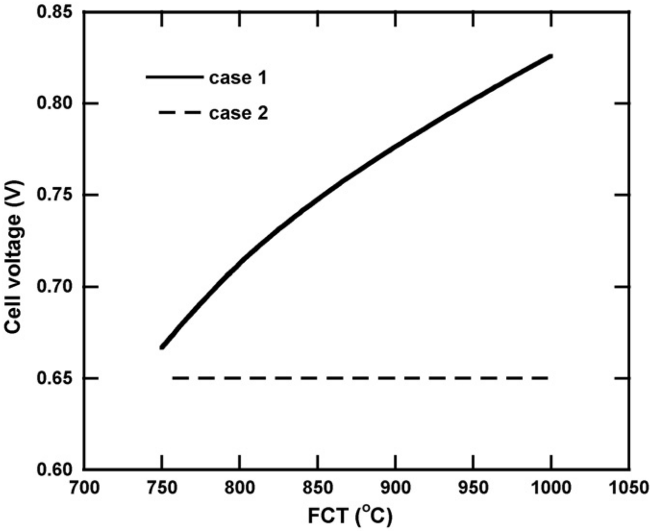

Fig. 2. Two cases of the cell voltage variation.

The Nernst potential is calculated from the theoretical Gibbs function difference for the electro-chemical reaction as usual. The activation polarization loss and the ohmic losses are predicted by correlations available in the literature [15,16]. The equation predicts increasing voltage with increasing cell temperature. An example of the prediction result is shown in Fig. 2. A constant current density (400 mA cm^{-2}) is assumed for all design conditions. In the second case, a constant cell voltage of 0.65 V is assumed, as also shown in the figure.

Several heat exchangers are used in the hybrid system and their effectiveness is defined as follows:

$$\varepsilon = \frac{T_{\mathrm{c,out}} - T_{\mathrm{c,in}}}{T_{\mathrm{h,in}} - T_{\mathrm{c,in}}} \tag{4}$$

The recuperator effectiveness is assumed to be the same as that of the original gas turbine cycle. The effectiveness of the preheater is variable. The absorbed heat of the cold side (air) at the preheater determines the temperature of the cathode inlet air (CIT). It is known that the cathode inlet temperature affects the system performance [3,9]. In general, if the current density is designed to be the same as given in the present study, a lower CIT for a given fuel cell operating temperature (FCT) enhances the performance, especially the power. However, an overly large temperature difference (rise) at the cell will cause mechanical problems mainly due to large thermal stress evolution inside the cell. In this work, a reasonable range for the temperature difference at the cell, defined as follows, is considered in order to examine its influence on the hybrid system design.

$$\Delta T_{\mathrm{c}} = \mathrm{FCT} - \mathrm{CIT} \tag{5}$$

Since the cell is modeled as a bulk control volume as other components, a single value of the cell operating temperature (FCT) is used. Also, the gas exiting from the cell is assumed to have this temperature. For each design case (different cell temperatures), the degree of air heating at the preheater, i.e. its effectiveness, is varied to meet the cathode inlet temperature.

The dc power generated at the fuel cell is calculated as follows:

$$\dot{W}_{\mathrm{FC,dc}} = VI = V(\dot{n}_{\mathrm{H_2}} + \dot{n}_{\mathrm{CO}})_{\mathrm{reacted}} 2F \tag{6}$$

The energy balances at the cell and the reformer are presented by the following equations:

$$\text{Cell}: \quad \sum_{\mathrm{in}} \dot{n}_i \bar{h}_i + \dot{Q}_{\mathrm{c}} = \sum_{\mathrm{out}} \dot{n}_i \bar{h}_i + \dot{W}_{\mathrm{FC,dc}}, \quad \text{where } \dot{Q}_{\mathrm{c}} < 0 \tag{7}$$

$$\text{Reformer}: \quad \sum_{\mathrm{in}} \dot{n}_i \bar{h}_i + \dot{Q}_{\mathrm{r}} = \sum_{\mathrm{out}} \dot{n}_i \bar{h}_i, \quad \text{where } \dot{Q}_{\mathrm{r}} = -\dot{Q}_{\mathrm{c}} \tag{8}$$

The final ac power from the SOFC is calculated as follows considering the dc to ac conversion loss.

$$\dot{W}_{\mathrm{FC,ac}} = \dot{W}_{\mathrm{FC,dc}} \eta_{\mathrm{conv}} \tag{9}$$

The gas turbine power is calculated as follows, assuming turbine and compressor efficiencies and other miscellaneous losses:

$$\dot{W}_{\mathrm{GT,ac}} = (\dot{W}_{\mathrm{T}} \eta_{\mathrm{m}} - \dot{W}_{\mathrm{C}}) \eta_{\mathrm{gen}} \tag{10}$$

Considering the auxiliary power consumption at the recirculation blower, fuel compressor, water pump and so on, the net hybrid system power and efficiency are described as follows:

$$\dot{W}_{\mathrm{HS}} = (\dot{W}_{\mathrm{FC,ac}} + \dot{W}_{\mathrm{GT,ac}} - \dot{W}_{\mathrm{AUX}}) \tag{11}$$

$$\eta_{\mathrm{HS}} = \frac{\dot{W}_{\mathrm{HS}}}{(\dot{m}\mathrm{LHV})_{\mathrm{CH_4}}} \tag{12}$$

The major design parameters for the SOFC and auxiliary parts are summarized in Table 2. Compared with the gas turbine only system, there exist additional pressure losses at the cell and the preheater. Commercial process analysis software [17] has been used in the simulation of this study.

Table 2
Design parameters of the SOFC and auxiliary parts

Fuel cell temperature	700–1050 °C
Temperature difference at the cell	100–200 °C
Fuel utilization factor at the cell	0.7
Steam carbon ratio	3.0
Heat exchanger effectiveness	0.75–0.83
Fuel compressor efficiency, water pump efficiency	0.75
dc to ac conversion efficiency	0.93
Pressure loss at the cell	3%
Recuperator pressure losses	Cold side 1.5%, hot side 2.5%
Duct pressure losses	0.5%

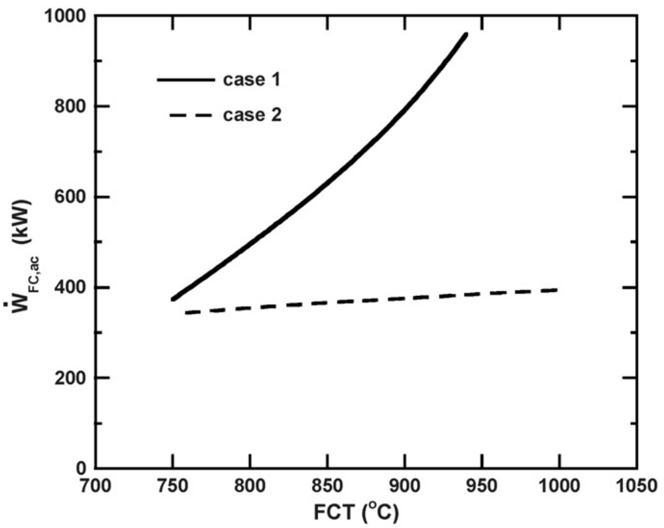

Fig. 3. Variation of the SOFC power with design cell temperature.

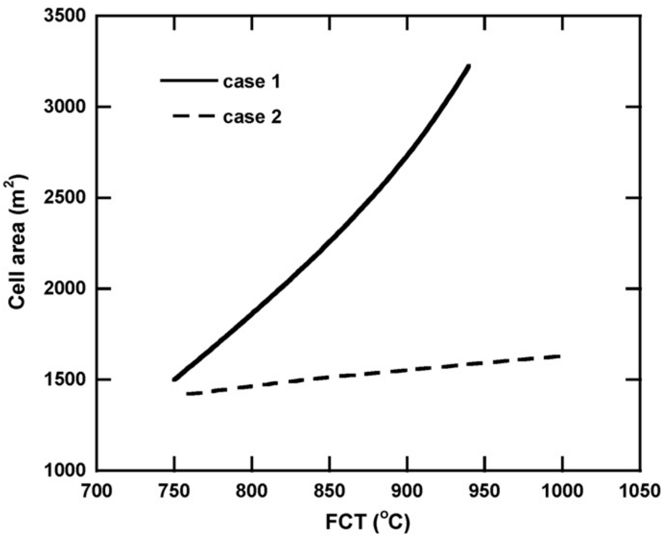

Fig. 4. Variation of the required effective cell area with design cell temperature.

3. Results and discussion

3.1. Design characteristics

The rotational speed of the gas turbine is fixed at the original design speed for all the hybrid system designs. For a fixed speed, various operating points of the gas turbine (more specifically those of the compressor) are possible according to different settings of design parameters of the SOFC and other parts. The major design parameters are those of the cell stack module such as the cell operating temperature, the cell voltage and the temperature difference at the cell. In this section, fundamental characteristics of a hybrid system design based on a fixed gas turbine design and the influence of the two aforementioned voltage cases on the system design and performance are discussed. In this section, a reference value of 150 °C is used for the temperature difference at the cell. The influence of its variation on the system design is addressed in the next section.

Fig. 3 shows the variation in the fuel cell power with the design cell temperature. As the design cell temperature increases, the operating pressure increases and the air flow rate decreases slightly as will be shown on the compressor map (Fig. 5). However, this slight change of pressure and air flow does not dramatically alter the cell performance. The most important factor affecting the SOFC performance variation is the design cell temperature. Increasing the design cell temperature enables a greater SOFC power. As clearly seen in the result of case 2, where a constant cell voltage is assumed, increasing cell temperature itself provides an increase in the cell power capacity. This is due to the increase in the fuel supply with increasing cell temperature to satisfy the energy balance at the cell, as described by Eq. (7). With an increase of the fuel supply, the heat release to the reformer also increases because the reforming heat is proportional to the fuel flow, and at the same time the enthalpy difference between the inlet and outlet streams also increases. If the cell voltage also increases with increasing cell temperature, as in case 1, the heat balance at the cell stack module allows much greater fuel supply to the cell. Consequently, the resulting cell power is far greater than that of the lower voltage case (case 2). As a result, the cell power increases by both the increased cell voltage and the increased fuel supply. Of course, the required design cell area should increase as the cell power increases as shown in Fig. 4, because the current density is assumed to be the same for all design cases, as explained earlier.

Fig. 5 describes various hybrid system design points on the compressor map corresponding to different design cell temperatures. All design conditions are located on the 100% speed line as explained. The left end point is the presumed surge point. The numbers in parentheses denote the design cell temperature and the corresponding turbine inlet temperature. The original gas turbine design point (1.0 kg s^{-1}) is also marked. The turbine inlet temperature is directly affected by the cell operating temperature, as can be readily surmised from the pressurized system layout. Thus, increasing cell temperature results in an increase

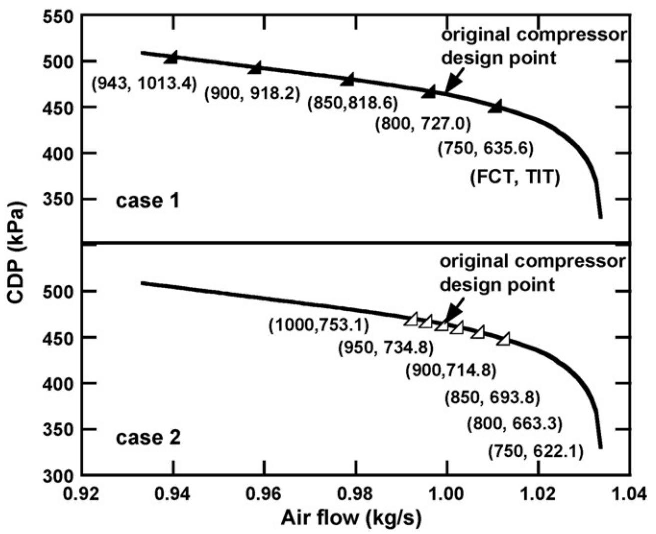

Fig. 5. Various design points on the compressor characteristic map depending on the design cell temperature ($\Delta T_c = 150$ °C).

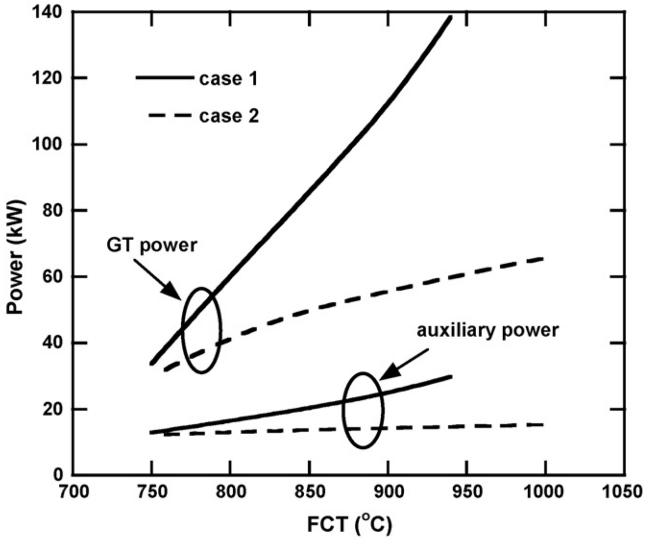

Fig. 6. Variation of the GT power and the auxiliary power with design cell temperature ($\Delta T_c = 150\,^{\circ}\mathrm{C}$).

of the turbine inlet temperature. The increase of the compressor discharge pressure, i.e. the pressure ratio of the compressor, with increasing turbine inlet temperature is a natural characteristic of the gas turbine. The higher the turbine inlet temperature is, the greater the net gas turbine power becomes. A distinct difference between the two voltage cases is that a higher cell voltage allows a higher turbine inlet temperature at the same design cell temperature. The higher cell voltage allows a larger fuel supply to the cell, as explained earlier. Thus, case 1 provides a higher turbine inlet temperature for a given cell temperature than case 2 does, because the fuel combusted at the afterburner also increases. Therefore, the design points of case 1 are located in a relatively higher pressure ratio range, while those of case 2 are located in the lower pressure ratio range.

Variations in the gas turbine power and the required auxiliary power consumption are shown in Fig. 6. As the design cell temperature increases, the turbine inlet temperature increases, and thus the gas turbine power also increases. The difference in the gas turbine powers of the two voltage cases is proportional to the difference in the turbine inlet temperatures between the two cases. In case 2, the maximum turbine inlet temperature at the maximum cell temperature design condition (1000 °C) is about 753 °C, far lower than the original design turbine inlet temperature (950 °C) of the gas turbine. Thus, the corresponding maximum gas turbine power (65 kW) in the hybrid system is also smaller than the original design power of the gas turbine (120 kW). In case 1, the maximum gas turbine power is comparable to the original power. However, the corresponding operating condition approaches the surge too closely. Therefore, the practical maximum power appears to be somewhat smaller than the original turbine power.

Accordingly, in both cases, the original turbine inlet temperature, and thus the original gas turbine power, is hard to achieve. This is equivalent to stating that the turbine inlet temperature of the hybrid system at every compressor operating condition is lower than the original turbine inlet temperature. As an example, the turbine inlet temperature at the original compressor design condition (mass flow rate of $1.0\,\mathrm{kg\,s^{-1}}$) is far lower than the design turbine inlet temperature (950 °C). This is more severe in case 2. In the pressurized hybrid system, many additional components are inserted between the compressor and the turbine compared with the original gas turbine only system. The main effect of the existence of these additional parts is an increase in the pressure loss. As the pressure loss between the compressor and the turbine increases, the turbine inlet pressure decreases. Thus, even if the compressor running point is the same (same compressor discharge pressure), the turbine inlet temperature must be lowered to satisfy the turbine characteristic (refer to Eq. (1)). In other words, in order to maintain the turbine inlet temperature close to the original temperature, the compressor discharge pressure increases and moves towards the surge line. This may explain the major cause of the near-surge problem in a previous experimental study [11] noted in the introduction. If the control logic of the gas turbine is not modified, the control system might try to attain the design turbine inlet temperature, which could be very close to the surge condition. Thus, for safe operation, the turbine inlet temperature needs to be de-rated from the original temperature.

The above analysis illustrates that it is difficult to obtain the original gas turbine power in the hybrid system, mainly due to the additional pressure loss at the fuel cell stack and piping. The additional pressure loss assumed in the current analysis for Figs. 2–7 is about 7% with respect to the compressor discharge pressure. If the hybrid system could be manufactured with less pressure loss than that assumed in this analysis, higher system performance would be obtained. On the contrary, further increase of the pressure loss would aggravate the situation.

A sample sensitivity analysis has been performed to examine the effect of the increased pressure loss at the cell on various performance indices. Results for case 1 are presented in Fig. 7. The design cell temperature is fixed at 850 °C and the pressure loss at the cell is doubled from 3 to 6%. Due to the additional pressure loss, the compressor discharge pressure increases by

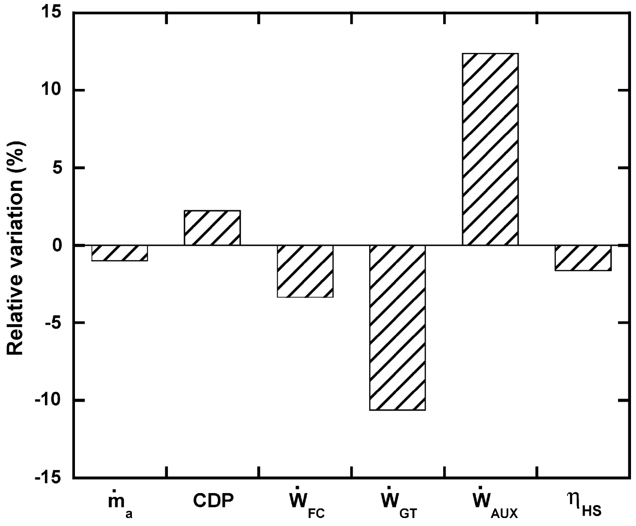

Fig. 7. Influence of an increase in pressure loss at the SOFC stack from 3 to 6% on various system parameters ($\Delta T_c = 150\,^{\circ}\mathrm{C}$).

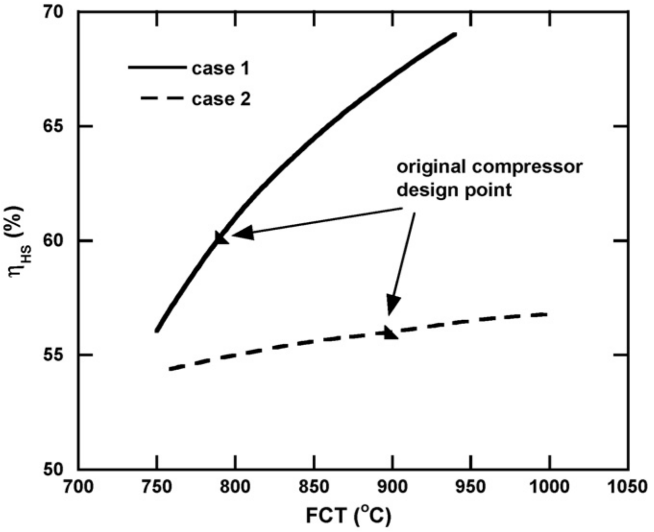

Fig. 8. Variation of the hybrid system efficiency with design cell temperature ($\Delta T_c = 150\,^{\circ}$C).

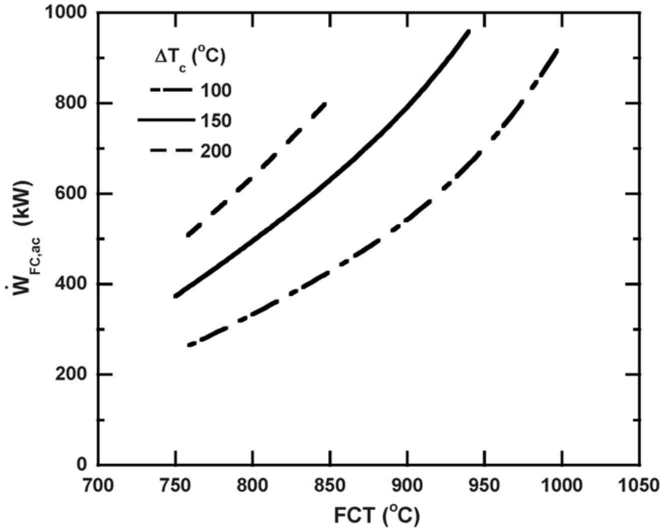

Fig. 9. Influence of the temperature difference at the cell on the SOFC power in case 1.

about 2%. The increased compressor pressure ratio requires larger compressor power consumption. Also, the pressure loss reduces the turbine power. Therefore, the net gas turbine power is reduced by more than 10%. The auxiliary power increases due to the increase in the power consumption of the recirculation blower. The SOFC power also decreases because the fuel supply is reduced according to the reduced air flow. As a result, the net hybrid system power is reduced by 5% and the system efficiency also decreases by more than 1%. The sensitivity analysis for case 2 produced almost equivalent results.

Fig. 8 shows the hybrid system efficiencies of the two cases. Even without the voltage increase, the system efficiency increases with increasing cell temperature as seen in case 2. If the voltage increases with increasing cell temperature (case 1), the system efficiency becomes far higher than that of the constant voltage case due to both the higher voltage itself and the accompanying greater addition of gas turbine power. A limitation of the higher voltage case is that a very high cell temperature (over 900 °C) is not very easy to design due to the surge problem noted previously. Considering this, the practical maximum hybrid system efficiency is about 65%. If the system design is more conservative, that is, if the original compressor design point needs to be maintained, i.e. the same surge margin is required, the design cell temperature is about only 790 °C and the system efficiency is about 60%. Therefore, the system efficiency depends substantially on the setting of the cell temperature, which in turn relies on the setting of the compressor operating point. In case 2, even though the overall system performance is lower than that of case 1, the surge problem is not as critical as in case 1 because the maximum cell temperature condition is sufficiently far from the surge point. Thus, the limiting design (1000 °C cell temperature) is achievable, leading to a maximum system efficiency of 57%. Since the efficiency does not vary extensively in case 2, the efficiency at the original compressor design point, where the cell temperature is about 900 °C, is as high as 56%. Consequently, although the theoretical maximum system efficiency differs considerably between the two voltages cases, the realistic system efficiency considering safe operation of the compressor does not differ greatly between the two cases.

3.2. *Influence of the temperature difference at the cell*

As briefly introduced in Section 2.2, the temperature difference at the fuel cell affects the system performance. Therefore, its influence on the design and performance of the current hybrid system needs to be examined. An analysis has been conducted for the two voltage scenarios with two additional temperature difference values (100 and 200 °C) and the results are presented together with that of the previous reference condition (150 °C). First, the results of case 1 are illustrated in Figs. 9–12. If ΔT_c is designed to increase for a given cell temperature, more fuel needs to be supplied. This allows larger cell power capacity as

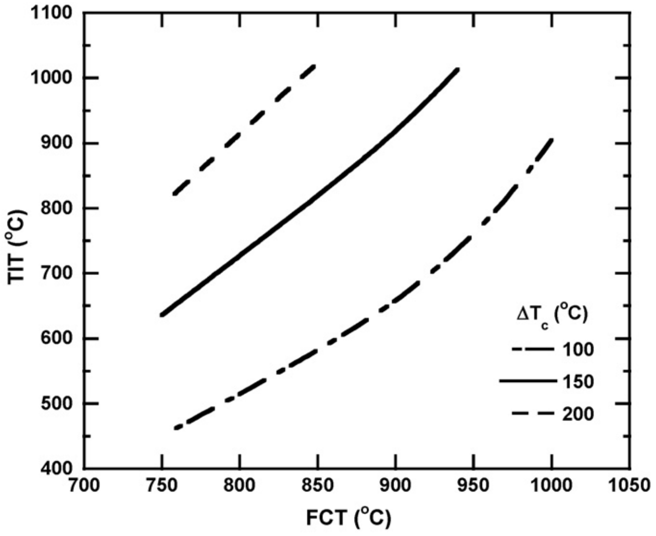

Fig. 10. Influence of the temperature difference at the cell on the turbine inlet temperature in case 1.

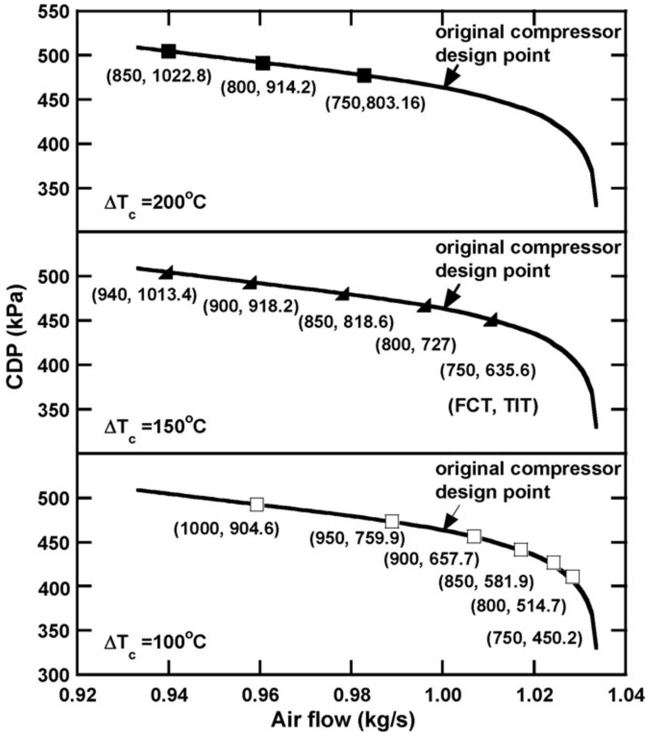

Fig. 11. Influence of the temperature difference at the cell on the operating condition of the compressor in case 1.

shown in Fig. 9. This also means that the redundant fuel after the cell reaction increases, resulting in an increase of the turbine inlet temperature as depicted in Fig. 10. The GT power is proportional to the turbine inlet temperature. The net effect of ΔT_c on the compressor operation condition is shown in Fig. 11. As examined in the previous section, the compressor operating condition is determined mainly by the turbine inlet temperature. Thus, since the turbine inlet temperature increases as ΔT_c increases, the compressor discharge pressure tends to increase (i.e., air flow decreases) with increasing ΔT_c for a given cell temperature. Consequently, even though a larger ΔT_c improves both the SOFC power and the GT power at a fixed cell temperature, it reduces the limiting (maximum allowable) cell temperature, considering the surge problem. In other words, the surge condition is approached with a lower cell temperature when the cell is designed with a larger ΔT_c.

System efficiencies are compared in Fig. 12. For a fixed cell design temperature, a design with a larger ΔT_c exhibits higher system efficiency due to the improved SOFC performance as well as the larger GT power. It is equivalent to say that a larger ΔT_c requires a lower cell temperature to obtain the same system efficiency. This result agrees with the previous analysis results [3,9], where no constraints on the compressor operation have been assumed. However, the results could be interpreted differently if we consider the practical limitation in the compressor operation. In the limiting operating condition close to the surge, the system efficiency of the design with a smaller ΔT_c is slightly higher. More generally speaking, when all designs should meet an equivalent surge margin, a smaller ΔT_c allows higher system efficiency due to a higher cell temperature. This can be illustrated by comparing the system efficiencies at the original compressor design points (i.e., with the same surge margin), also marked in the figure.

The influence of ΔT_c on the system design with a constant cell voltage (case 2) is illustrated in Figs. 13–16. All results are qualitatively similar to those of case 1. The major difference is that the maximum cell temperature (1000 °C) can be designed for all ΔT_c values in this low cell voltage case because the turbine inlet temperatures are far lower than those of case 1 for all corresponding design conditions, and thus the surge problem does not occur for all designs. With the smallest ΔT_c (100 °C), even the original compressor design point cannot be achieved, that is, the turbine inlet temperatures are very low. This results in negative gas turbine power for all conditions. Therefore, with a low cell voltage (0.65 V), ΔT_c of 100 °C does not provide any synergetic hybrid system design. Thus, if the design cell voltage

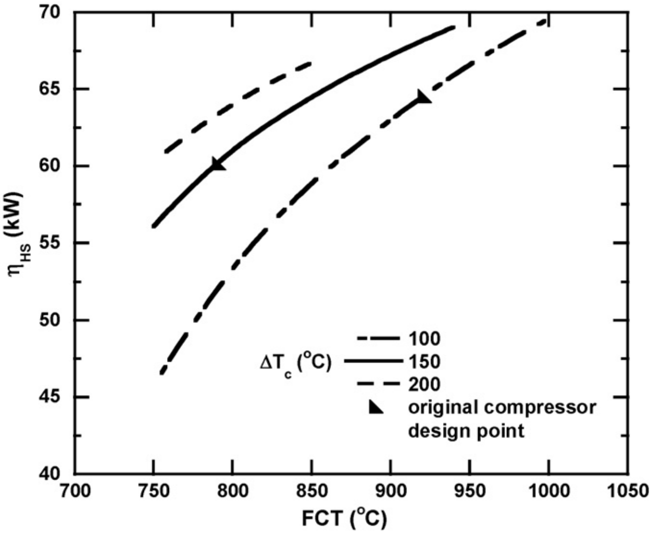

Fig. 12. Influence of the temperature difference at the cell on the hybrid system efficiency in case 1.

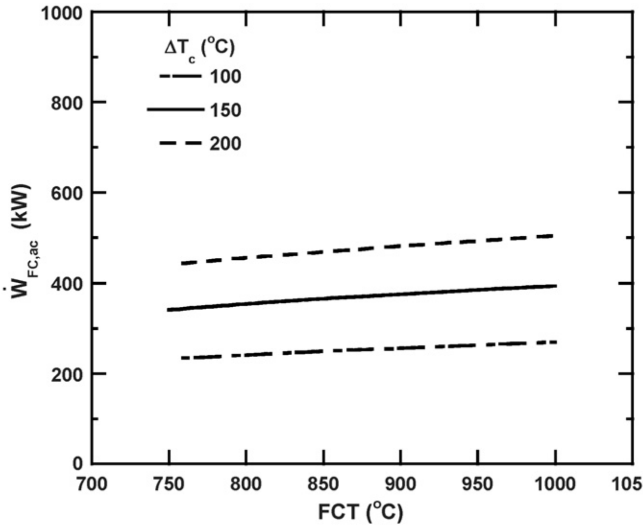

Fig. 13. Influence of the temperature difference at the cell on the SOFC power in case 2.

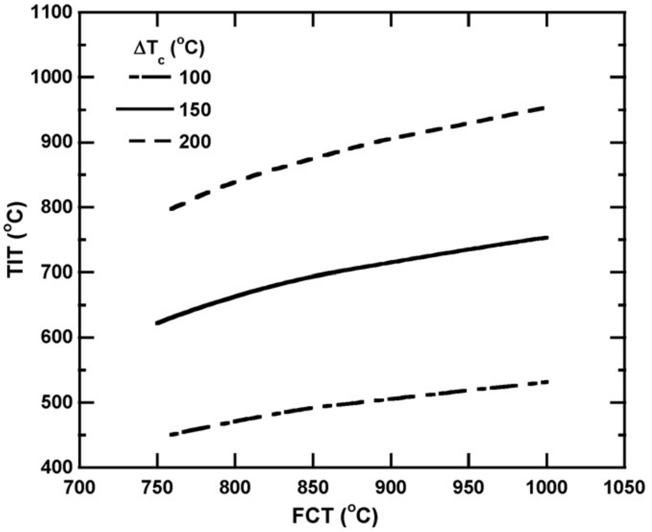

Fig. 14. Influence of the temperature difference at the cell on the turbine inlet temperature in case 2.

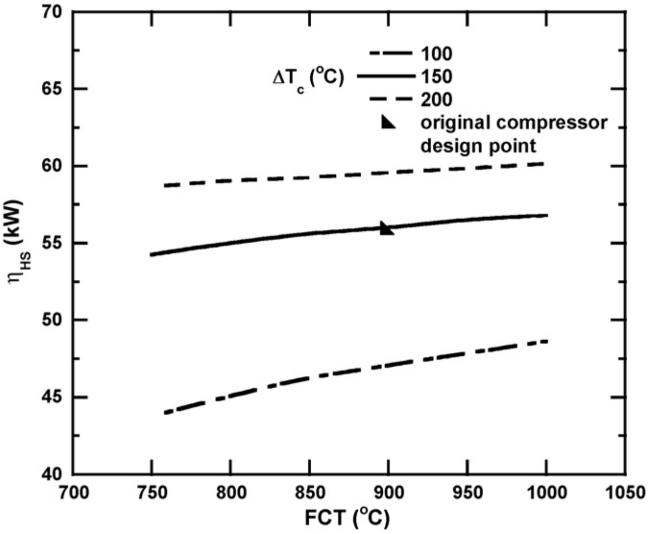

Fig. 16. Influence of the temperature difference at the cell on the hybrid system efficiency in case 2.

is lower, a larger temperature difference at the cell is required to achieve a hybrid system exploiting the synergetic combination of the SOFC with the GT. Remembering that the smallest ΔT_c in case 1 fully enables hybrid system designs for a wide cell temperature range, it can be concluded that a higher cell voltage allows wider design options in terms of the temperature difference at the cell. The lower cell voltage results in lower system efficiency when the design cell temperature is the same. However, if a design with an equivalent practical surge margin (the original design point of the compressor for example) is considered, the system efficiency difference between case 1 and case 2 is substantially reduced.

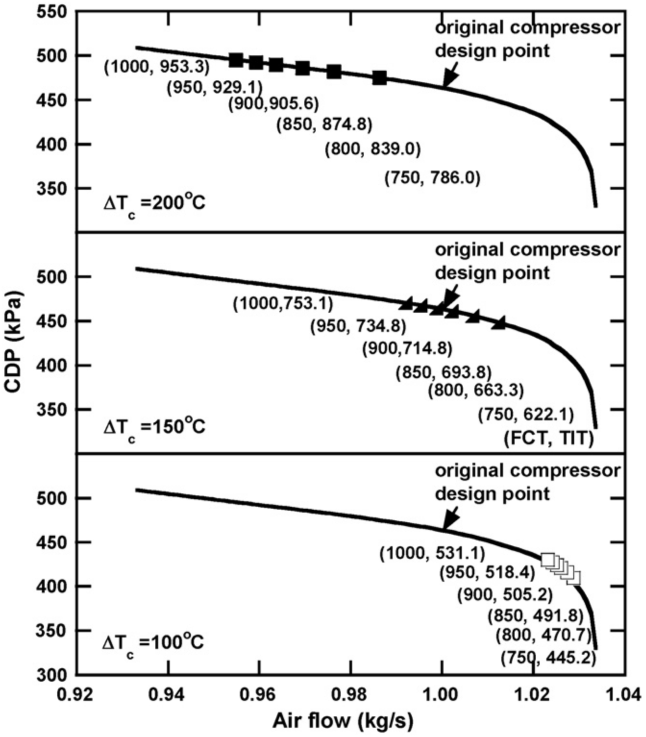

Fig. 15. Influence of the temperature difference at the cell on the operating condition of the compressor in case 2.

4. Conclusions

This study has simulated design of a pressurized SOFC hybrid system based on a fixed gas turbine design. The results are summarized as follows:

(1) As the design cell temperature increases, both the turbine inlet temperature and the pressure ratio increase, and system power and efficiency also increase. Due to the existence of pressure loss at the fuel cell, the turbine inlet temperature at the original design point of the compressor is lower than the design turbine inlet temperature. Thus, at the original compressor design point, the produced gas turbine power is far lower than the design power. The original design power level of the gas turbine can be obtained only at extreme operation conditions close to compressor surge.
(2) At a fixed cell temperature, a higher cell voltage provides not only larger SOFC power but also larger gas turbine power due to a higher turbine inlet temperature, and thus enables higher system efficiency. However, considering an equivalent surge margin (designed at the same compressor operating point), the design cell temperature needs to be lower as the cell voltage is higher. Thus, if the operating limitation of the compressor is fully taken into account, the efficiency advantage obtained with a higher cell voltage may be lessened.
(3) For a fixed design cell temperature, a larger temperature difference at the cell provides a larger gas turbine power with the same cell temperature, thus providing higher system efficiency. However, if the system is to be designed with an equivalent surge margin of the compressor, a larger temperature difference at the cell may exhibit lower sys-

tem efficiency because the cell temperature needs to be far lowered to meet the surge margin.

(4) A higher cell voltage allows a wider design options in terms of the temperature difference at the cell than a lower voltage does. In particular, if the cell voltage is low, the cell should be designed to have a sufficient temperature difference in order to achieve a meaningful hybrid system efficiency advantage over the fuel cell only system.

References

[1] M.C. Williams, J.P. Strakey, W.A. Surdoval, J. Power Sources 143 (2005) 191–196.

[2] B.H. Bae, J.L. Sohn, S.T. Ro, ASME Paper FUELCELL2003-1735.

[3] S.K. Park, T.S. Kim, J. Power Sources 163 (2006) 490–499.

[4] S.E. Veyo, L.A. Shockling, J.T. Dederer, J.E. Gillett, W.L. Lundberg, Trans. ASME: J. Eng. Gas Turbines Power 124 (2002) 845–849.

[5] G.D. Agnew, M. Bozzolo, R.R. Moritz, S. Berenyi, ASME Paper GT2005-69122, 2005.

[6] D. Bohn, N. Poppe, J. Lepers, ASME Paper GT-2002-30112, 2002.

[7] S. Campanari, ASME Paper GT2004-53933, 2004.

[8] E.A Liese, R.S. Gemmen, ASME Paper GT 2003-38566, 2003.

[9] W.J. Yang, T.S. Kim, J.H. Kim, J.L. Sohn, S.T. Ro, J. Power Sources 160 (2006) 462–473.

[10] T.W. Song, J.L. Sohn, T.S. Kim, S.T. Ro, J. Power Sources 158 (2006) 361–367.

[11] D. Tucker, L. Lawson, R. Gemmen, ASME Paper GT2005-68784, 2005.

[12] A. Hildebrandt, M. Assadi, ASME Paper GT2005-68744, 2005.

[13] S.L. Dixon, Fluid Mechanics, Thermodynamics of Turbomachinery, 3rd ed., Pergamon Press, 1978.

[14] J.J. Lee, J.E. Yoon, T.S. Kim, J.L. Sohn, J. Mech. Sci. Technol. 21 (2007) 141–152.

[15] S. Nagata, Y. Kasuga, A. Momma, T. Kato, Bull. Electrotechnol. Lab. Jpn. 5–6 (1993).

[16] A.F. Massardo, F. Lubelli, Trans. ASME: J. Eng. Gas Turbines Power 122 (2002) 27–35.

[17] Aspen Technology, AspenOne HYSYS, ver 2004.02, Aspen Technology, Inc., 2004.